JOURNAL OF MATERIALS SCIENCE 33 (1998) 2825–2830

Spatial–OH impurity distribution in gallium phosphate crystals

E. MARINHO, D. PALMIER, A. GOIFFON, E. PHILIPPOT*
Laboratoire de Physicochimie de la Matière Condensée, Université de Montpellier II, Place E. Bataillon, case courier 003, 34095 Montpellier cedex 5, France
E-mail: ephilip@lpmc.univ-montp2.fr

Piezoelectric properties of quartz and quartz-like materials are strongly related to the impurity content in the crystals and, more especially, to their hydroxyl group (–OH) content. This work has been devoted to the determination of the spatial distribution of this impurity in as-grown crystals of gallium phosphate, $GaPO_4$. The investigation was undertaken by infrared spectroscopy from eight samples with different growth conditions and completed by thermally stimulated current/relaxation map analysis techniques. The results allow the best growth parameters to be defined, leading to crystals with the lowest –OH impurity content.

1. Introduction

Infrared spectroscopy has long been used to characterize water molecules and hydroxyl groups bound to cations in ores [1–9]. To prevent drastic decrease of piezoelectric properties of materials like α-quartz and its homeotypes (berlinite, $AlPO_4$ and gallium phosphate, $GaPO_4$), the OH content must be minimized [10–15]. Solving this problem implies accurate determination of their OH content and understanding their mode of incorporation.

For quartz crystals, a careful study was first developed by Kats [16] for hydrogen incorporation and, subsequently, much work has been devoted to this problem and its influence on physical properties [17–24]. Large OH contents also affect the ductility of quartz [25–27]. In view of the strong similarities between properties and behaviour of α-quartz and its homeotypes, similar studies to those of α-quartz have been extended to them [14, 15, 28–31].

Previous studies have demonstrated the importance of the OH defects for piezoelectric applications of α-quartz and its homeotypes. Results obtained from infrared spectrometry are strongly related to many factors: sample crystallographic orientation, beam polarization, surface state, temperature, etc. All these parameters are not always specified and make difficult any comparison between results. On the other hand, many equations are proposed to quantify the OH content, but some ambiguities exist between them.

Within the framework of our work on $M^{III}X^{V}O_4$ (M = Al, Ga, Fe; X = P, As) quartz-like materials, we first determined growth conditions for high-quality berlinite and gallium phosphate crystals [14, 15]. Then, a relation was proposed in order to give an estimate of the OH amount existing in these as-grown materials [12].

Unfortunately, this relation does not give an absolute value of the OH content. Thus, relying on previous work on α-quartz and berlinite, we have tried to describe the spatial distribution of the OH groups for some $GaPO_4$ crystals obtained with typical growth parameters (different acid solvents and their concentrations, different growth temperatures, etc.). This investigation was completed by thermally stimulated currents/relaxation map analysis (TSC/RMA) which is a new and well-adapted technique for qualitative investigation of impurities such as OH groups.

2. Previous relations for α-quartz and berlinite

Infrared spectrometry, in the range 4000–2600 cm^{-1}, is the most suitable technique for semi-quantitative determination of the OH content in crystals. For quartz, Dodd and Fraser [17] considered the absorption coefficient, α, at 3500 cm^{-1} corresponding to the centre of the wide absorption band due to the OH groups in synthetic quartz. This α coefficient is given by the formula

$$\alpha_{3500} = \left(\frac{1}{d_{cm}}\right)\left(\log\frac{T_{3800}}{T_{3500}}\right) \quad (1)$$

where d is the sample thickness (cm) and T_{3800} the transmittance at 3800 cm^{-1} in a region not affected by OH absorption (background). Under these conditions, the [OH] content is related to the α value by the formula $[OH]_{ppm} = 90.90\,\alpha_{3500}$.

*Author to whom all correspondence should be addressed.

For berlinite, Steinberg *et al.* [12] proposed a slightly different estimate with an α-value given by the relation

$$\alpha_{3290} = \left(\frac{1}{d_{cm}}\right)\left(\log \frac{T_{3800}}{T_{3290}}\right) \quad (2)$$

where the absorption band at 3290 cm^{-1} is characteristic of OH groups associated with both Al^{3+} and P^{5+} cations of close atomic weights. Thus, the [OH] content is given by the relation $[OH]_{ppm} = 48.73\alpha_{3290}$.

3. Relations for gallium phosphate

For $GaPO_4$, two different ways have been adopted to express the hydroxyl content. In the absorption range characteristic of OH groups, the infrared spectrum of $GaPO_4$ exhibits three bands at 3400, 3290 and 3170 cm^{-1}, Fig. 1.

Krempl *et al.* [32] use the transmittance value at 3400 cm^{-1}

$$\alpha_{3400} = \left(\frac{1}{d_{cm}}\right)\left(\log \frac{T_{3800}}{T_{3400}}\right) - \alpha^* \quad (3)$$

where α^* is the absorbance at 3400 cm^{-1} which is not due to OH vibrations (usually 0.04). Indeed, for these authors, the two absorbance peaks at 3167 and 3290 cm^{-1}, after subtraction of the broad OH band, are independent of [OH] and only very weakly dependent on polarization. They attribute these two bands to third-order vibrations of the undisturbed $GaPO_4$ lattice which shows strong lattice bands at 2130 and 2240 cm^{-1}. In fact, these third-order vibrations would absorb at 3195 and 3360 cm^{-1} and then can also be superimposed on the OH absorption at 3400 cm^{-1}.

According to the berlinite measurements [12], we have chosen the transmittance values characteristic of OH groups linked to phosphorus (3290 cm^{-1}) and to the heaviest gallium atom (3167 cm^{-1}) as shown in Fig. 1. Then, the α-value is

$$\alpha = \left(\frac{1}{d_{cm}}\right)\left(\log \frac{T_{3800}}{T_{3170}} + \log \frac{T_{3800}}{T_{3290}}\right) \quad (4)$$

If Equation 3 is true, our values are then overestimated because we measured the OH content and the lattice absorbance simultaneously. Nevertheless, before checking Krempl's hypothesis, we can use our measurements for comparative studies of OH distribution in $GaPO_4$ crystals.

For the OH content, Krempl *et al.* [32] used the formula $[OH]_{p.p.m.} = 65\alpha_{3400}$. The factor 65 is derived from the water in fused silica [16]. In our case, only the α-values are given.

4. Experimental procedure and results

The spatial infrared investigation of eight different gallium phosphate crystals was undertaken and the comparative α-values were computed from both Equations 3 and 4. The aim of this study was to determine the OH content of each sample versus the distance from the seed, on the basis of multiple infrared measurements, and to map its contour lines with constant α values, called "iso-α" lines.

As shown in Fig. 2, as-grown crystals were obtained from *X*- and *Z*-seeds and themselves can be sawn in *X*- or *Z*-slices. From the four possible different ways, two for each kind of crystal, we only retained the *Z*-slices whatever the initial seed used in the growth experiment. In these conditions, *Z*-slices from *X*-seed crystal contain the initial seed in their middle. On the other hand, *Z*-slices from *Z*-seed crystal are parallel to the initial seed. If *x*, *y* and *z* coordinates of any point are easy to define for *Z*-slices of *X*-seed crystal (seed trace), it is more difficult in the other case where the only marker is the *Y*-axis trace, Fig. 2.

From this methodology, the "iso-α" cartography was realized for all the crystals obtained with different growth conditions. For this purpose, the *Z*-slices and their orientations must be carefully located after sawing and polishing. The last step is to criss-cross meticulously each slide in such a way that all squares (2 mm × 2 mm), with the same *x* and *y* coordinates, are rigorously overlapped, Fig. 3. The good coincidence is checked by superposing all slices of the same crystal.

In preliminary experiments, with a DA8 Bomem FT spectrometer, the nature of the OH impurity was

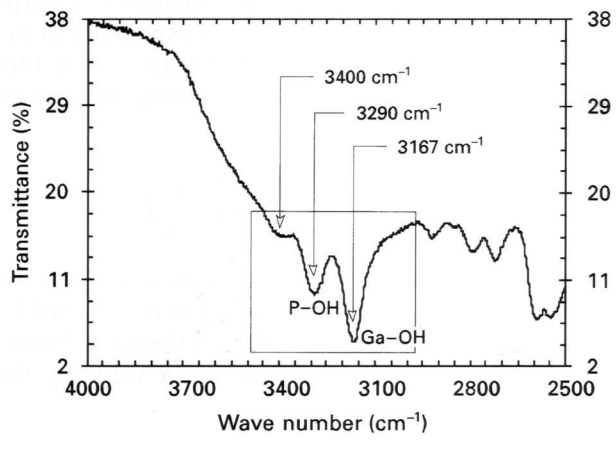

Figure 1 Typical infrared spectrum of $GaPO_4$ in the range 4000–2500 cm^{-1}.

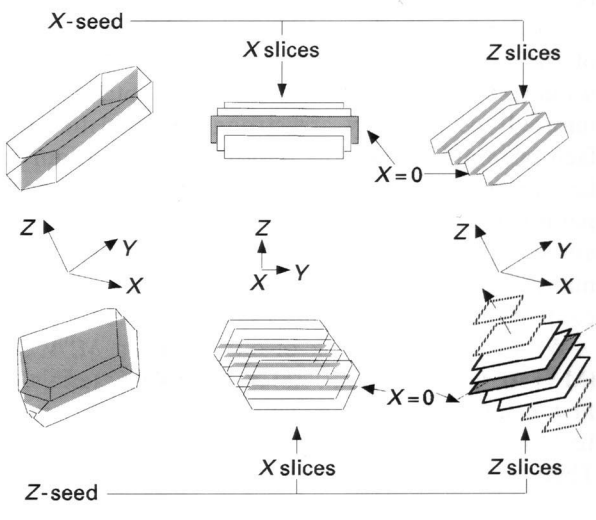

Figure 2 Schematic drawing of the four different ways of cutting (2 *X*- and 2 *Z*-slices) from *X*- and *Z*-seed crystals.

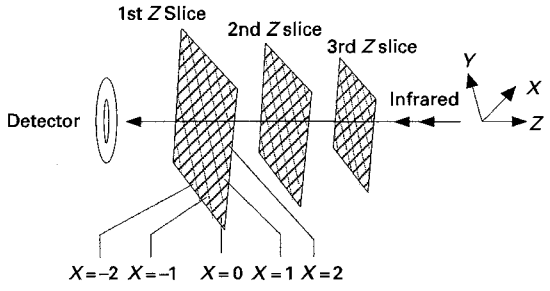

Figure 3 Example of three adjacent Z-slices from Z-seed crystal with their overlapping square pattern.

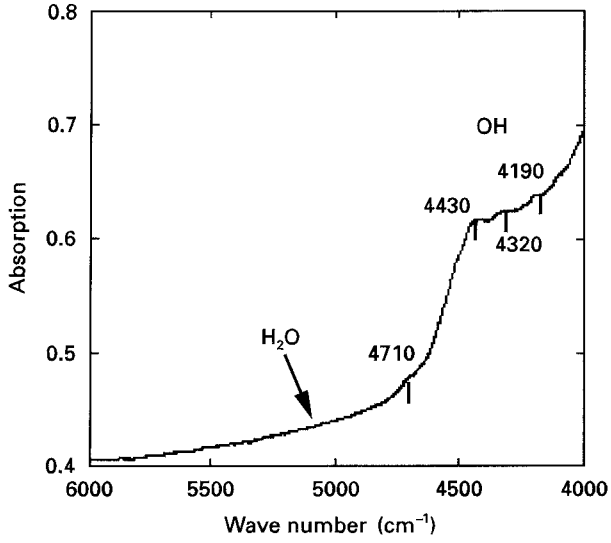

Figure 4 Near infrared spectrum of a $GaPO_4$ crystal showing the absence of molecular water.

checked by near infrared spectrometry which can differentiate OH groups (four bands in the range 4200–4700 cm^{-1}) and molecular water (band at 5200 cm^{-1}). On the contrary, for berlinite crystal [31], molecular water was never observed in $GaPO_4$ crystals, whatever the growth conditions, Fig. 4.

The spectrometer used for infrared investigation was a Fourier transform Perkin–Elmer 1600. As summarized in Table I, samples are obtained from crystal growth in sulphuric acid (X-seeds, concentration 6 mol l^{-1} and crystal growth temperature, $T_c = 200$ and 220 °C). The α-values have been computed following either Equation 4, our approximation (α_{total}, including both absorption bands at 3170 and 3290 cm^{-1}), or Equation 3 (α, taking into account only the mean value at 3400 cm^{-1}), with $(\alpha_{total}/\alpha) = 3$. Fig. 5a–d summarize some of the most characteristic evolutions of the α-values in two- and three-dimensional representations. Each contrast corresponds to a constant α-value area with a difference of the α-value of 0.5 cm^{-1} between two adjacent contour lines. The resulting α-values for only one characteristic section of each crystal are reported in Table I. From these results, an extrapolated final α-value can be computed via the relation

$$\alpha_{extrap} = \frac{a}{(bx^4 + cx^3 + dx^2 + e)^f} - \frac{g}{(hx^2 + i)^j} + k \quad (5)$$

TABLE I Evolution of the extinction coefficient, α, in a plane parallel to the seed for various crystals of gallium phosphate obtained in sulphuric and phosphoric acids (the italic values of α correspond to the value calculated from Equation 3)

Solvent	Concentration, C (mol l^{-1})	T (°C)	Seed	α (cm^{-1}) at										
				−7.5 mm	−5.0 mm	−3.0 mm	−2.5 mm	−2.0 mm	−1.0 mm	0.0 mm	+1.0 mm	+2.0 mm	+2.5 mm	+3.0 mm	+5.0 mm	+7.0 mm
H_2SO_4	6.00	200	X	–	2.64	–	2.44	–	–	4.55	–	–	1.51	–	1.30	–
					0.85		*0.77*			*1.61*			*0.39*		*0.31*	
		230	X	1.87	2.06	–	1.84	–	–	3.45	–	–	1.81	–	1.80	1.95
				0.52	*0.59*		*0.51*			*1.14*			*0.49*		*0.49*	*0.55*
H_3PO_4	9.00	150	X	–	–	–	2.30	–	–	2.57	–	–	2.43	–	–	–
							0.46			*0.56*			*0.51*			
	14.80	150	X	–	6.49	–	5.55	–	–	5.42	–	–	5.93	–	7.99	–
					2.12		*1.75*			*1.69*			*1.90*		*2.71*	
			Z	–	–	–	–	9.00	7.66	4.52	11.01	8.04	–	6.23	–	–
								3.00	*2.42*	*1.07*	*3.86*	*2.59*		*1.81*		
		200	Z	–	–	–	–	1.01	1.16	1.47	1.19	1.12	–	–	–	–
								0.17	*0.22*	*0.32*	*0.23*	*0.21*				
	15.75	163	X	–	–	–	6.88	–	–	6.58	–	–	6.16	–	–	–
							2.02			*1.94*			*1.82*			
	16.70	200	Z	–	–	0.90		0.81	1.08	1.25	1.22	<0.68	–	–	–	–
						0.00		*0.00*	*0.14*	*0.29*	*0.28*	*0.00*				

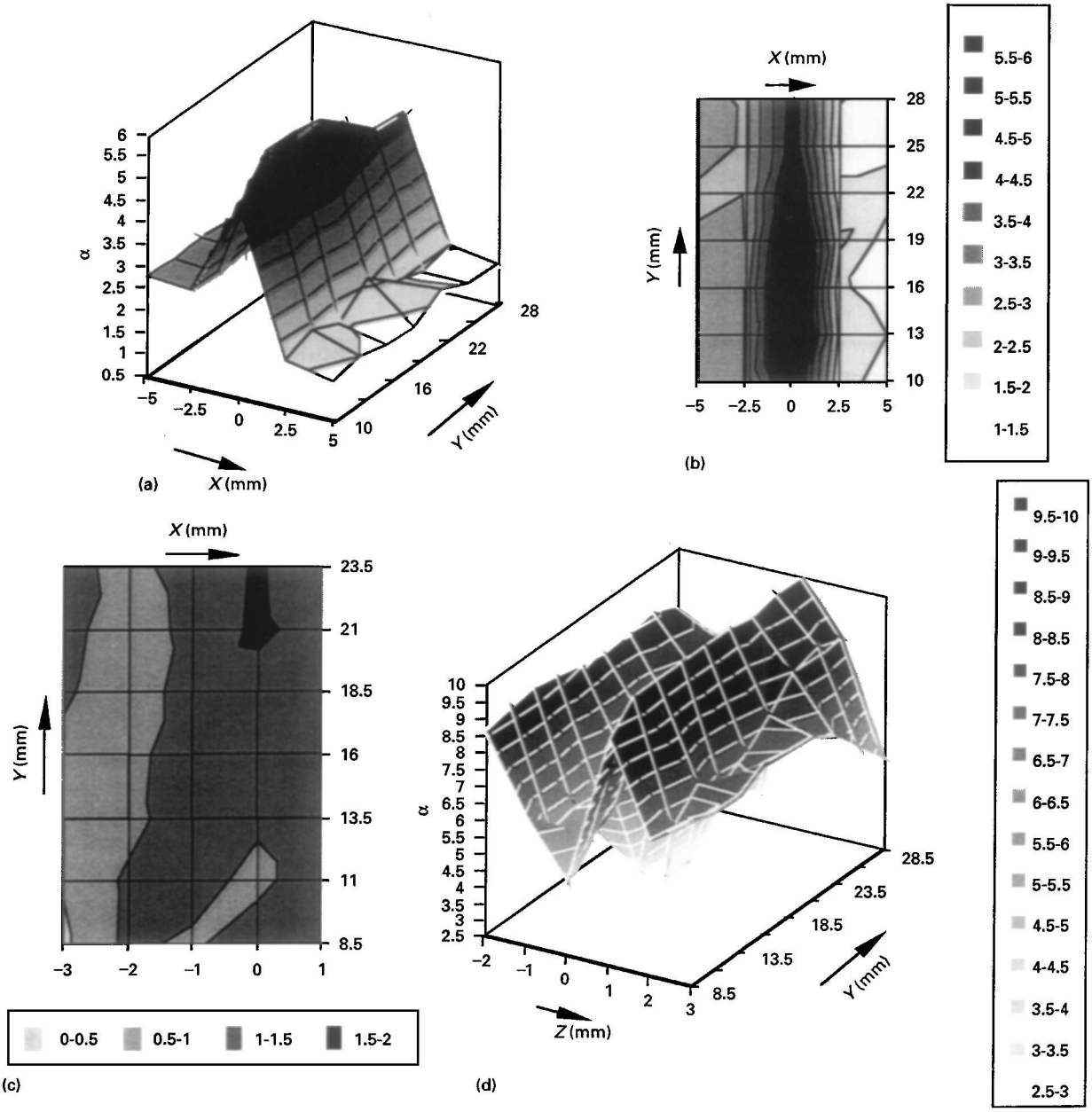

Figure 5 Some examples of OH content distribution in $GaPO_4$ crystals: (a) three-dimensional evolution of the α-value for an *X*-seed crystal (H_2SO_4 6 mol l^{-1}, T_c =200 °C); (b) two-dimensional evolution of the α-value for the same crystal; (c) two-dimensional evolution of the α-value for a *Z*-seed crystal with low OH content (H_3PO_4 16.7 mol l^{-1}, T_c = 200 °C); (d) three-dimensional evolution of the α-value for a *Z*-seed crystal (H_3PO_4 14.8 mol l^{-1}, T_c = 150 °C) with bad restart conditions.

where x is the abscissa (mm, distance from the seed) and $a, b, \ldots, k$ are constants, refined by least square refinement, Fig. 6 (non-continuous observed variations are generally due to crystal defects).

Another way to characterize the hydroxyl groups is the TSC/RMA technique which is able to follow the relaxation of thermally stimulated molecules in a high and continuous electrical field. This method is especially well adapted to insulating materials such as gallium phosphate crystals. Fig. 7 shows the TSC spectra of crystals obtained at different growth temperatures. The first intensity maximum, in the low-temperature range (− 50–0 °C) is due to the change between a "frozen" state (all the OH dipoles, oriented in the applied field direction, are "frozen" at low temperature), and a "disordered" state (when an increase of temperature leads to a "disordered" distribution of these dipoles). The first experiments allow us to correlate, using a linear relation, the current intensity and the α-value computed from infrared spectrometry, Fig. 8. In other words, the depolarization current is linearly related to the OH content. Explanation of the second intensity maximum at higher temperatures (50–150 °C) is not so easy, but it may be related to electrode effects or other kinds of impurities, such as small moving cations. This TSC method, connected to infrared measurements, seems to be promising to the search for knowledge of the hydroxyl group behaviour in materials such as gallium phosphate crystals and, from a more general point of view, quartz [33] and its homeotypes. On the other hand, the TSC/RMA method will perhaps be able to relate impurity content to the second intensity peak at higher temperature.

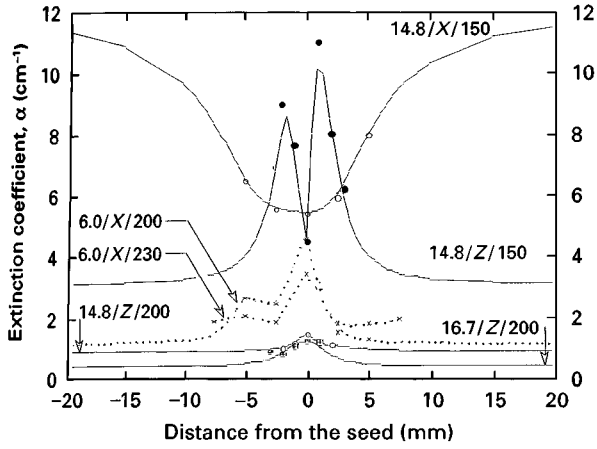

Figure 6 Mean α-value evolution for more characteristic samples of $GaPO_4$ in (– – –) sulphuric and (——) phosphoric solvents. The three values for each sample are the acid concentration, the seed orientation and the growth temperature. The theoretical evolution has been fitted by Equation (5).

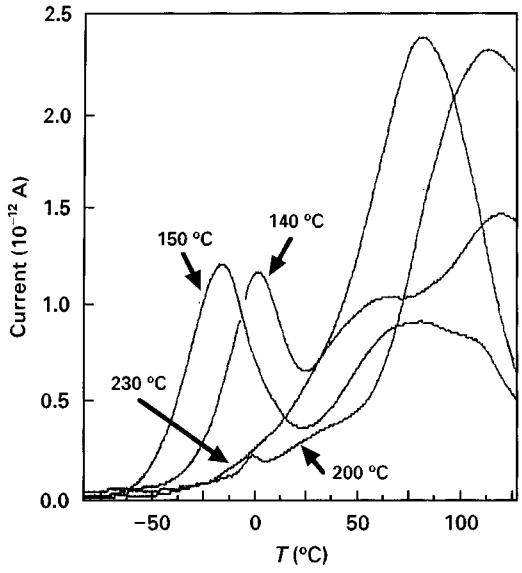

Figure 7 Depolarization current for various *Z*-slices of crystals obtained in phosphoric acid 14.8 mol l^{-1} (140 and 150 °C) and sulphuric acid 6 mol l^{-1} (200 and 230 °C).

5. Discussion

In view of the different initial α-values of the seeds, the final extrapolated ones have been considered as the intrinsic characteristics in terms of growth parameters: temperature, T_c, solvent conditions and temperature gradient between cold and hot zone, ΔT [14, 15]. First, if we consider the ΔT influence, all other parameters being constant, its increase accelerates the convection current and thus the growth rate and the OH content [15]. For the same growth conditions, the α-value is much more important for *X*-seed crystals than for *Z*-seed ones (14.8/*X*/150 and 14.8/*Z*/150) in accordance with faster *X* growth rates ($0.1 < V_x < 0.2$ mm/d.face) than *Z* ones ($0.01 < V_z < 0.02$ mm/d.face), Fig. 6. The initial strong increase of the OH content near the seed in 14.8/*Z*/150 crystal is characteristic of bad restart conditions, as already observed for berlinite crystals, $AlPO_4$ [14].

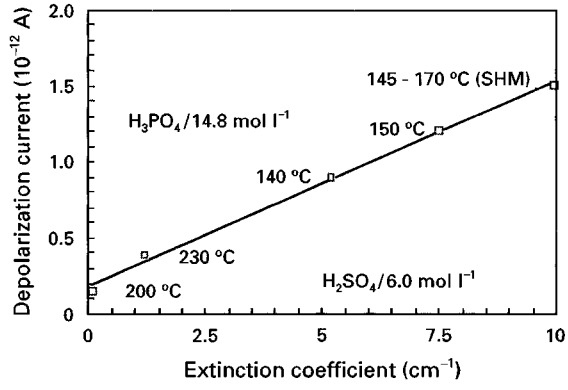

Figure 8 Evolution of the depolarization current in terms of the α-value extinction coefficient (SHM, crystal growth by the slow heating method between 145 and 170 °C).

Concerning the influence of solvent, we can observe that the OH content increases with the acid concentration, and thus with the H_3O^+ concentration. For the first strong acidity of phosphoric acid

$$H_3PO_4 + H_2O \rightleftharpoons H_2PO_4^- + H_3O^+ \qquad (6)$$

In this medium, another parameter favours a higher OH content at "lower" temperature. Indeed, the reaction enthalpy of the process $H_2O + HPO_4^{2-} \rightarrow PO_4^{3-} + H_3O^+$ is 13.419 kJ mol^{-1} at 150 °C, but decreases to −0.77 kJ mol^{-1} at 200 °C [34]. Thus, for low growth temperatures, the high concentration of HPO_4^{2-} species favours OH groups.

From a general point of view, all experiments in an acid concentration less than or equal to 9 mol l^{-1} for phosphoric acid and 6.0 mol l^{-1} for sulphuric acid, lead to a rather weak final α-value, whatever the growth temperature ($\alpha \lesssim 3$ cm^{-1}). On the contrary, for a high concentration of solvent and a fast growth rate, the final OH content can be greater than that of the *X*-seed (14.8/*X*/150).

In brief, whatever the crystal growth parameters, the V_z growth rate is always weak ($V_z \leq 0.04$ mm/d.face) and, thus, crystals from *Z*-seeds always show low OH content. This result is in accordance with previous work on berlinite crystals [14]. The major difference between $AlPO_4$ and $GaPO_4$ crystals is an OH content much smaller for $GaPO_4$, all crystal growth parameters being similar [14, 15]. Thus, if for berlinite, low α-values are obtained with $T_c \geq 230$ °C, for $GaPO_4$, the same α-values are obtained with $T_c \geq 200$ °C in highly concentrated acidic phosphoric solutions (16.7/*Z*/200).

6. Conclusion

The spatial study of the OH distribution in $GaPO_4$ crystals by infrared spectrometry has shown that this impurity is not uniformly distributed inside the crystal. Generally, the OH content first decreases when the distance perpendicular to the seed increases and then becomes constant beyond about 5 mm. On the contrary, the OH content is the same in a plan parallel to the seed.

From *X* seeds, the only possibility to grow $GaPO_4$ crystals with a low OH content is to use a sulphuric

acid medium. Unfortunately, as previously observed in this solvent [15], the V_z growth rate is very weak and, so, the crystal growth process leads to crystals not suitable for an industrial application.

On the other hand, in phosphoric acid media, the V_z value increases and the V_x growth rate is still good enough. Moreover, in this medium, whatever the growth conditions, crystals from Z-seeds exhibit a low OH concentration. Thus, this solvent seems to be the most promising for future development.

Acknowledgements

The authors thank the DGA/DSP and the CNRS for their financial support.

References

1. D. L. WOOD and K. NASSAU, *J. Chem. Phys.* **47** (1967) 2220.
2. R. W. T. WILKINS and W. SABINE, *Am. Mineral.* **58** (1973) 508.
3. S. GOLDMAN, G. R. ROSSMAN and W. A. DOLLASE, *ibid.* **62** (1977) 1144.
4. A. BERAN and A. PUTNIS, *Phys. Chem. Mineral* **9** (1983) 57.
5. R. D. AINES and G. R. ROSSMAN, *J. Geophys. Res.* **89**(B6) (1984) 4059.
6. A. BAUMER, M. GANTEAUME and W. E. KLEE, *Bull. Mineral.* **108** (1985) 145.
7. A. BERAN, *Phys. Chem. Minerals* **13** (1986) 306.
8. F. FREUND and G. OBERHEUSER, *J. Geophysic. Res.* **91**(B1) (1986) 745.
9. J. INGRIN, K. LATROUS, J. C. DOUKHAN and N. DOUKHAN, *Eur. J. Mineral.* **1** (1989) 327.
10. B. SAWYER, *IEEE Trans. Sonics Ultras.* **19**(1) (1972) 40.
11. R. A. LAUDISE and R. L. BARNS, *IEEE Trans. Ultras. Ferroelect. Freq. Control* **35**(3) (1988) 277.
12. R. F. STEINBERG, M. K. ROY, A. K. ESTES, B. H. T. CHAI and R. C. MORRIS, in "Proceedings of the IEEE Ultrasound Symposium" (Institute of Electrical & Electronics Engineers, Piscataway, USA, 1984) p. 279.
13. R. S. FALCONER, J. F. VETELINO and B. H. T. CHAI, in "IEEE Ultrasound Symposium" (Institute of Electrical & Electronics Engineers, Piscataway, USA, 1985) p. 241.
14. E. PHILIPPOT, A. GOIFFON, M. MAURIN, J. DÉTAINT, J. C. SCHWARTZEL, Y. TOUDIC, B. CAPELLE and A. ZARKA, *J. Crystal Growth* **104** (1990) 713.
15. E. PHILIPPOT, A. IBANEZ, A. GOIFFON, M. COCHEZ, A. ZARKA, B. CAPELLE, J. SCHWARTZEL and J. DÉTAINT, *ibid.* **130** (1993) 195.
16. A. KATS, *Philips Res. Repts* **17** (1962) 133.
17. D. M. DODD and D. B. FRASER, *J. Phys. Chem. Solids* **26** (1965) 673.
18. D. CHAKRABORTY and G. LEHMANN, *J. Solid State Chem.* **17** (1976) 305.
19. *Idem, Phys. Status Solidi* **34** (1976) 467.
20. *Idem, Z. Naturforsch.* **33a** (1978) 290.
21. M. HOSAKA, S. TAKI, K. NAGAI and J. ASAHARA, in "Proceedings of the 35th Annual Frequency Control Symposium" (Institute of Electrical & Electronics Engineers, Piscataway, USA, 1981) p. 304.
22. M. S. PATERSON, *Bull. Mineral.* **105** (1982) 20.
23. R. D. AINES, S. H. KIRBY and G. R. ROSSMAN, *Phys. Chem. Minerals* **11** (1984) 204.
24. H. G. LIPSON, F. EULER and A. F. ARMINGTON, in "Proceedings of the 40th Annual Frequency Control Symposium" (Institute of Electrical & Electronics Engineers, Piscataway, USA, 1986) p. 11.
25. M. S. PATERSON and K. R. S. S. KEKULAWALA, *Bull. Mineral* **102** (1979) 92.
26. A. K. KRONENBERG, S. H. KIRBY, R. D. AINES and G. R. ROSSMAN, *J. Geophys. Res.* **91**(B12) (1986) 12723.
27. P. CORDIER and J. C. DOUKHAN, *Eur. J. Mineral.* **1** (1989) 221.
28. J. C. DOUKHAN, B. BOULOGNE, P. CORDIER, E. PHILIPPOT, J. C. JUMAS and Y. TOUDIC, *J. Cryst. Growth* **84** (1987) 167.
29. B. BOULOGNE, P. CORDIER and J. C. DOUKHAN, in "1st European Frequency and Time Forum" (Printing Office of Conseil Général du Doubs, Besançon, France, 1987) p. 209.
30. P. CORDIER, B. BOULOGNE and J. C. DOUKHAN, *Bull. Mineral* **111** (1988) 113.
31. J. M. DURAND, A. IBANEZ, A. GOIFFON and E. PHILIPPOT, *J. Solid State Chem.* **109** (1994) 106.
32. P. W. KREMPL, F. KRISPEL, W. WALLNÖFER and G. LEUPRECHT, in "Proceedings of the 9th European Frequency and Time Forum" (Printing Office of Conseil Général du Doubs, Besançon, France, 1995) p. 66.
33. C. POIGNON, G. JEANDEL and G. MORLOT, *J. Appl. Phys.* **80** (1996) 6192.
34. J. GOMES MORALES, R. RODRIGUEZ CLEMENTE, J. DURAND and L. COT, *J. Cryst. Growth* **128** (1993) 1250.

Received 18 June 1997
and accepted 13 February 1998